2013 IEEE/RSJ International Conference on
Intelligent Robots and Systems (IROS)
November 3-7, 2013. Tokyo, Japan

Force-Position Control for a Miniature Camera Robotic System for Single-Site Surgery

I. Rivas-Blanco, E. Bauzano, M. Cuevas-Rodríguez, P. del Saz-Orozco and V.F. Muñoz, *Member, IEEE*

Abstract— **This paper describes the design and implementation of a robotic vision system for single-site surgery. The system is composed of a wireless miniature camera robot with magnetic pan and tilt capabilities, and an external robotic arm to guide the camera along the abdominal wall. The camera robot is provided with a set of magnets, and a magnetic holder is attached at the end effector of the manipulator. This way, the camera robot can be displaced to obtain additional viewpoints of the abdominal cavity by displacing the external manipulator. The first prototype of the camera robot with an embedded LED lighting system is described. To properly displace the robotic arm over the abdominal wall, a hybrid force-position control has been developed, which includes a torque compensation module in order to obtain an appropriate orientation of the end effector. The contact surface has been assumed to be an elastic model, which stiffness matrix is estimated with a recurrent least squares algorithm. Finally, an in-vitro experiment to validate the control scheme proposed is presented.**

I. Introduction

Nowadays minimally invasive surgery is a widely accepted technique all over the world, not only by surgeons but also by patients, who benefit from its esthetical advantages derived from the small incisions whereby surgeons operate. Compared with open traditional surgery, laparoscopic techniques offer the advantages of reducing the invasiveness, including reduction of intraoperative blood loss, tissue trauma, risk of post-operative infection, pain experienced by the patient and recovery time [1]. The natural next step for laparoscopic surgery seems to be reducing to one the number of incisions. In this sense, single-site surgery (also known as single incision laparoscopic surgery) is a new alternative in which all of the laparoscopic working ports enter the abdominal wall through the same incision. Benefits of this new generation method include less incisional pain, better patient's recovery thanks to lower postoperative narcotic requirements and faster return to normal life, improved cosmetics, and higher patient satisfaction [2]. Despite these advantages, single-site surgery techniques have some challenges that cannot be overlooked. Close proximity of the laparoscope and instruments, as they are sharing the same port, entails a loss of triangulation between the camera and the working ports, and limits the range of motion [3]. This fact reveals the need of using special semiflexible or curved laparoscopic instruments, so that a larger space can be achieved without crashing tools. The use of these new instruments makes necessary specific skills training periods for surgeons to be comfortable with them, even for experienced surgeons in traditional laparoscopy [4]. Flexible endoscopes are composed of a flexible shaft and bending tip, which angle of deflection is controlled by means of navigation wheels. Handling of flexible endoscopes requires combining various actions to perform the desired movements, which results really complex for surgeons [5]. New generation of teleoperated flexible endoscopes are presented in [6].

An alternative to overcome these problems is addressed by inserting a miniature robot into the abdominal cavity. This way, the number of instruments sharing the port is reduced, and the loss of degrees of freedom (DOF) due to the fulcrum effect is avoided. Moreover, by placing a camera into the robot, it can be moved apart from the surgical tools, avoiding the problem of the loss of triangulation and providing additional camera angles by displacing the camera along the abdominal wall. The positioning and fixation of these robots to the abdominal wall is done by suturing [7], by needle locking [8]-[10], and by external magnets placed on the abdominal wall, as in [11] or [12]. Many studies have addressed the approach of using external magnets to guide and anchor internal devices [13]-[18]. Lehman et al. [19] proposed a miniature robot with two arms with unfold and refold capabilities, which are anchored to the abdominal wall via magnetic interaction. In Simi et al. [20], a wired miniature vision platform based on a magnetically activated robot is proposed. The fixation of the robot to the abdominal wall is done with a set of external permanent magnets, moved by hand. A similar conception is used in [21], where the internal unit consists of an actuated triangular-shaped magnetic frame which allows the anchoring of several robotic units at the same time. In Terry et al. [22], an internal device is fixed to the entry port access through a rigid ring and cantilever bar, or by an external magnetic handle.

In this paper, we present a wireless miniature camera robot with magnetic pan and tilt capabilities, and magnetic anchoring to the abdominal wall. Unlike previous work, external magnets are attached to the end effector of a robotic arm, so guidance of the camera is done automatically by displacing the external manipulator. The advantage of this approach is that the movement of the camera can be controlled by a human machine interface, such a voice commands, which avoids the need of direct manipulation by the surgeon or an assistant. Moreover, autonomous strategies to move and orientate the camera can be developed. Furthermore, the design of the actuation of the tilt and pan DOFs along with the inclusion of batteries makes it possible to have a completely wireless device. To properly displace the robotic arm over the abdominal wall, preventing damages

This work was supported in part by the Spanish national project DPI2010-21126.

I. Rivas-Blanco, E. Bauzano, M. Cuevas-Rodríguez, P. del Saz-Orozco and V.F. Muñoz are with the department of Systems Engineering and Automation, University of Malaga, Spain (Corresponding author to provide phone +34 952132540; fax +34 952131413; e-mail: vfmm@uma.es).

due to excessive forces, a force position control with torque compensation has been developed.

This paper is organized as follows. Description of the robotic system and specific design of the camera robot is presented in section II. Section III illustrates the force-position control with torque compensation to guide the external magnets over the abdominal wall. Experimental results, along with a recurrent least squares algorithm to estimate the environment stiffness matrix are reported in section IV. Finally, conclusions are discussed in section V.

II. Miniature Camera Robotic System

The system proposed in this work consists of a wireless miniature camera robot, which is inserted into the abdominal cavity through the entry port, and a robotic arm where a magnetic holder is attached (Fig. 1). The internal device is provided with a set of magnets, so once inside the abdomen, it can be fixed to the abdominal wall by magnetic interaction with the magnetic holder. As the magnetic holder is attached to the end effector of a robotic arm, guidance of the camera robot is done by displacing the manipulator. This way, the camera robot can be moved away from the entry port, avoiding the problem of the loss of triangulation due to the proximity of the camera and the surgical tools. Furthermore, as the camera can be moved along the abdominal wall, more camera angles than with traditional laparoscopes can be obtained, providing the surgeon with additional viewpoints of the abdominal cavity. To achieve an appropriate guidance of the camera robot along the abdominal wall, both movement along the tangents directions of the surface at the contact point ($\vec{t}$) and force along the normal direction ($\vec{n}$) must be controlled. A hybrid force-position control with torque compensation is discussed in section III. Next the camera robot design is described.

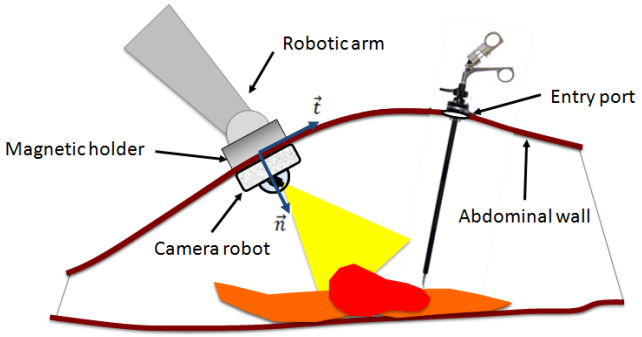

Figure 1. Robotic system overview

The camera robotic system is composed of three parts: the miniature camera robot, a magnetic holder, and a wrist attachment component (Fig. 2). Coupling between the wrist attachment and the magnetic holder allows the possibility of releasing the magnetic holder once the camera robot has been placed in a desired location. This way, several miniature robots can be handled by the same manipulator. Moreover, this system allows both automatic guidance with a manipulator or dragging the camera robot by hand motion of the magnetic holder. Miniature camera robot has two DOF to orientate the camera towards different areas of the abdomen: pan and tilt. Pan motion is obtained by rotating the nth joint of the manipulator, as the internal magnets of the camera robot follow the movement of the magnetic holder. The tilt DOF is actuated by a linear motor in the wrist attachment component, which displaces component A in Fig. 3. This shaft component is coupled with the cone-shaped piece B, which has a small magnet at the bottom. This piece is stuck to the internal magnet C of the magnetic holder. Displacement of magnet C causes a displacement of a cylindrical magnet (D) located inside the camera robot, which is connected to the camera and therefore provokes a change in its inclination. This way, the actuation of the motor generates a tilt motion of the camera, which allows a variation of ±42º in the camera angle.

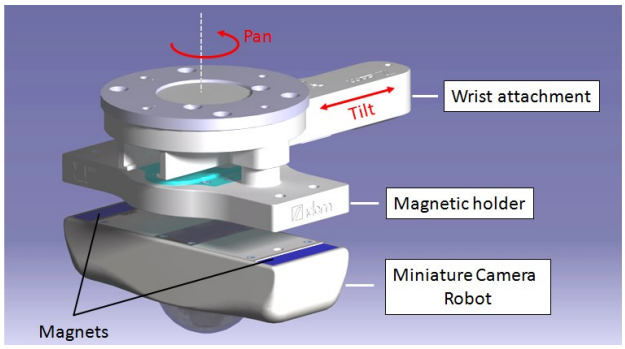

Figure 2. Robotic camera design

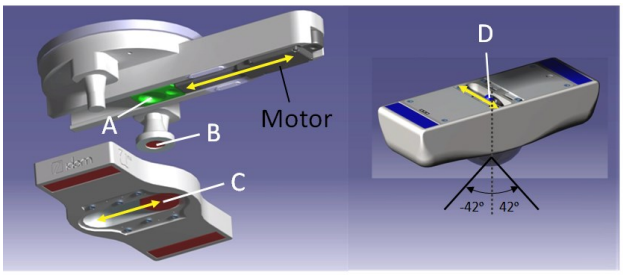

Figure 3. Tilt DOF

Fig. 4 shows the first functional prototype of the miniature camera robot of dimensions 12 cm length by 4 cm width. Future works will include a new design of the robot to reduce its overall size. A wireless camera is used to acquire the images of the abdominal cavity, which are transmitted to an external receiver. Additionally to tilt and pan motion, software zoom can be used to focus the image on a smaller

Figure 4. First miniature camera robot prototype

area. To illuminate the scene, a set of six white LEDs are distributed around the camera, each emitting 6.8 candela with a 20 mA current. Seven 9 volts batteries (250mAh) are used to supply the power required by the camera and the LEDs system, avoiding the need of wires to supply the system. The autonomy of the system is around 4 hours, which is enough for a usual minimally invasive procedure, as a cholecystectomy.

III. Force-Position Control with Torque Compensation

A force-position control is developed in order to provide an appropriate interaction force between the magnetic holder and the abdominal wall while displacing the robot. The complete control scheme is depicted in Fig. 5. A *task planner* generates the force and position references required to control the system. Position reference (P_r) specifies a desired position along the tangent directions of the surface ($\vec{t}$) at the contact point, while force reference (F_r) sets the desired force along the normal direction ($\vec{n}$). This way, force and position control actions are decoupled through matrices *D* and *I-D*, avoiding problems of interferences between the two controllers. As depicted in Fig. 5, a hybrid force-position control is used to track force and position references with parallel *force* and *position controllers*. In order to maintain the manipulator orientation perpendicular to the surface, a *torque compensation* module with null reference for the desired torque is included in the control scheme, aimed at reorientating the robot during the movement. This module is necessary due to the fact that directions $\vec{t}$ and $\vec{n}$ are time-variant, as the abdominal wall is not a flat surface. An *orientation controller* is used to obtain an accurate orientation tracking. As the end effector is maintained perpendicular to the surface during the movement of the manipulator, task reference frame is assumed to be coincident with the end effector reference frame ${}^0R_n$, where {0} is the robot base frame and *n* represents the nth joint of the manipulator. This rotation matrix is used to transform positions and orientations in the task reference to the robot base frame, and vice versa. Next, details of the hybrid force-position control and the torque compensation module are described.

A. Hybrid Force-Position Control

Force controller translates a force reference into a position reference along the normal direction (P_N), which added to the reference in the tangents directions (P_T) provides a unique position reference ${}^0P_n$ to the robot. For the force controller design, an elastic interaction model between the robot and the surface has been assumed:

$$F = K_x \Delta P_N \tag{1}$$

Where K_x represents the environment stiffness matrix, and ΔP is the compression amount. If force error ΔF represents the difference between the force reference and the measured force, equation (1) yields to:

$$\Delta F = K_x\big(P_N(\Delta t) - P_N(t)\big) \tag{2}$$

Therefore, the required position to exert a force of ΔF on the surface is derived as follows:

$$P_N(\Delta t) = P_N(t) + \Delta F \cdot \frac{1}{K_x} \tag{3}$$

On the other hand, position controller assures an accurate position reference tracking. This is done with a PI controller of gains K_P and K_I according to equation (4), where P_r is the position reference and *e(t)* is the position error.

$$P_T(\Delta t) = P_r + K_P P_T(t) + K_I \int e(t)dt \tag{4}$$

Robot dynamics is forced to follow a first order behavior [23], so PI gains are designed following the Ackerman's methodology for poles assignment, according to a dead-beat strategy:

$$K_P = \frac{1+e^{-(T/\tau)}}{1-e^{-(T/\tau)}} \;;\; K_I = \frac{1}{e^{-(T/\tau)}-1} \tag{5}$$

Where T is the system sampling time and τ is the time constant.

B. Torque Compensation

Torque compensation, depicted in Fig. 6, is aimed at maintaining the orientation of the robot perpendicular to the surface at the contact point. Torques at the end effector are generated when the contact force is not uniformly distributed along the sensor surface. In such a case, the force vector forms an angle α with the end effector z axis. So the goal of the torque compensation module is to keep axis ${}^0z_n$ parallel to the force vector, which is always normal to the contact surface. To compensate the torques generated when the end effector is not perpendicular to the surface, a rotation by an angle of α in the opposite direction of the torque vector is applied. Rotation angle and direction are calculated in the *geometric model* module of Fig. 6. Once the rotation matrix is obtained, it is transformed into robot base frame coordinates by means of the rotation matrix ${}^0R_n$. Gain K_τ in Fig. 6 assures an accurate tracking of the null torque reference.

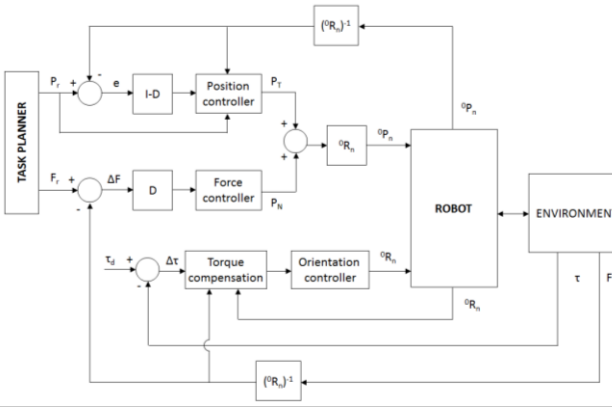

Figure 5. Complete force-position control scheme

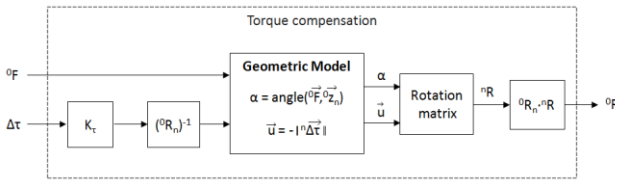

Figure 6. Torque compensation module

Once the desired orientation of the robot has been established, an *orientation controller* is used to assure a correct tracking of the orientation reference. To this end, a quaternion-based controller depicted in Fig. 7, has been designed. The desired orientation, output by the torque compensation module in form of a rotation matrix, is transformed into a desired quaternion q_d. A relation between joint velocities $\dot{\theta}$ and the time derivative of the quaternion representing the orientation of the robot can be established by means of an appropiate analytical Jacobian matrix $J_A(q)$ as follows:

$$\dot{q} = J_A(q)\dot{\theta} \tag{6}$$

Considering q_e as the difference between the desired quaternion q_d and the actual one:

$$q_e = q_d - q \tag{7}$$

As q_d is a constant value, equations (6) and (7) yields to:

$$\dot{q}_e = -J_A(q)\dot{\theta} \tag{8}$$

Defining the control law as $\dot{\theta} = (J_A(q))^T K_q \mathrm{q_e}$, the system is asymptotically stable, being K a positive definite symmetric matrix [24]. Furthermore, a quaternion planner is included in order to provide a smooth orientation transition. Quaternion interpolation is done according to the spherical linear interpolation (SLERP) method [25].

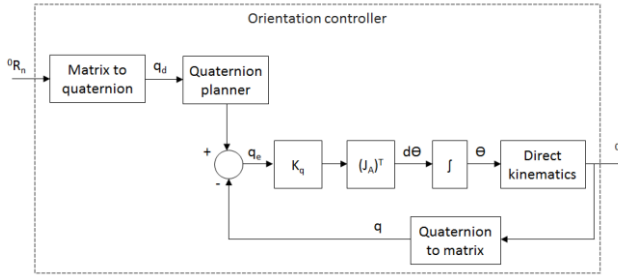

Figure 7. Quaternion-based Orientation Controller

IV. Experiments and Results

A. System implementation

In order to verify the proposed control scheme, an in-vitro experiment consisting on displacing the camera robot along the *y* direction while exerting a force along the *z* direction has been carried out. The experiment set-up is depicted in Fig. 8. A methacrylate box of dimensions 46 cm x 36 cm x 26 cm simulates the abdominal cavity, with a neoprene layer at the top to simulate an elastic model of the contact surface. Further work will include experiments with non-flat surfaces and mannequin-like models. Guidance of the camera robot along the surface is done with a 7 DOF Barrett WAM robotic arm. This cable-driven robot exhibits zero backlash with low friction and low inertia, endowing the WAM with good open-loop "backdrivability" [26], which makes it possible to move the end effector by hand to a desired location and makes it inherently safe for humans. Furthermore, this robot can be directly operated in the Cartesian domain, avoiding the need of inverse kinematics calculations. Interaction force and torque between the manipulator and the surface are obtained

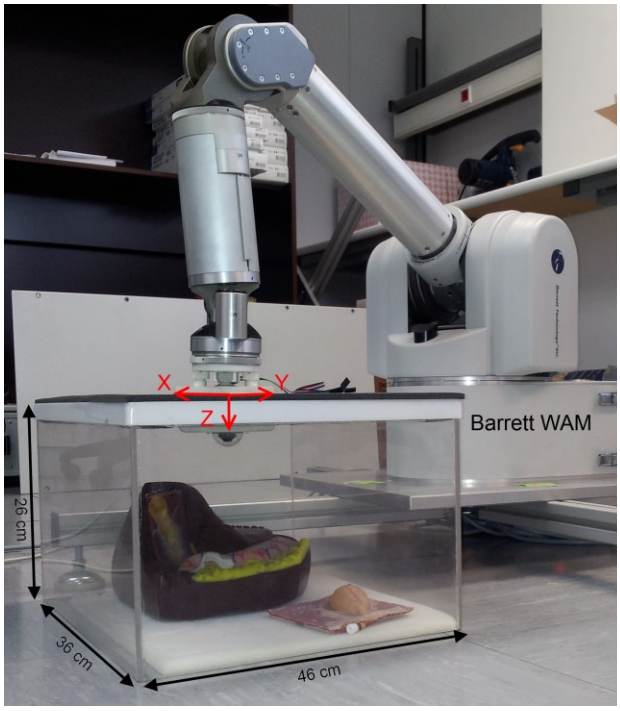

Figure 8. System implementation

by means of a self-contained 6-axis force-torque sensor [27]. To guarantee the stability of the complete control scheme, force, position and orientation controllers have a smaller sampling time than its input references, in order to assure a steady-state of the robot before a new reference is sent [28].

The control scheme described in section III has been implemented in ROS, an open-source framework specifically designed for robotic applications [29]. This software platform makes it possible to easily integrate several sensing and actuation systems in the same computer. The main advantage of using ROS in our particular application is the possibility of sending and receiving information to and from the robot and the motor which controls the camera tilt DOF with a unique interface. This way, an easy interaction with the whole system can be achieved. Likewise, additional devices can be effortlessly integrated in the system.

B. K_x estimation

For the force controller design, the environment (abdominal wall) has been assumed to be an elastic model. The estimation of the stiffness matrix is done with a recurrent least squares algorithm (RLS). This method employs measures of position and force obtained during the normal working of the system to update the stiffness matrix value K_x in real time. Previously to the operation, the external manipulator is placed by hand on the patient's abdominal wall, and pressured to exert a force. K_x is estimated with the data acquired during the process, and the value obtained is used in the force controller during the movement of the camera robot. This way, particular characteristics of each patient's abdominal wall are taken into account in the stiffness value calculation.

Let $F_z(t)$ and $z(t)$ be the z-component of the measured force and position with respect to the task frame in a time instant, respectively. Equation (2) leads to:

$$F_z(t) - F_z(t-1) = k_3(z(t) - z(t-1)) \quad (9)$$

Where k_3 represents the third diagonal component of the stiffness matrix. First and second diagonal components of K_x are null as x and y position components does not contribute to the force exerted on the surface. Defining force and position increments as $\Delta F = F_z(t) - F_z(t-1)$ and $\Delta z = z(t) - z(t-1)$ equation (9) can be rewritten as follows:

$$\Delta F = k_3 \Delta z \quad (10)$$

Where n represents the number of values measured, and k_3 is the parameter to be estimated. Assuming known the estimated stiffness value at instant N, $\hat{k}_3(N)$, the estimated value at instant N+1, $\hat{k}_3(N+1)$, is calculated by correcting $\hat{k}_3(N)$ with the new data measured:

$$\hat{k}_3(N+1) = \hat{k}_3(N) + R(N)\left(\Delta F(N+1) - \Delta z(N+1)\hat{k}_3(N)\right) \quad (11)$$

Where:

$$R(N) = \frac{Q(N)\Delta z(N+1)}{1+\left(\Delta z(N+1)\right)^2 Q(N)} \quad (12)$$

And variable Q is updated as:

$$Q(N+1) = \frac{Q(N)}{1+\left(\Delta z(N+1)\right)^2 Q(N)} \quad (13)$$

The RLS algorithm is initialized at $N=0$. Estimated $\hat{k}_3$ value and variable Q at the initial time are defined as:

$$\hat{k}_3(0) = \frac{\Delta F(0)}{\Delta z(0)} \quad (14)$$

$$Q(0) = \frac{1}{\left(\Delta z(0)\right)^2} \quad (15)$$

To validate the reliability of the algorithm proposed, a set of three experiments consisting on measuring the end effector position while exerting a force on the surface have been carried out. Results are depicted in Fig. 9, where noise due to the small quantities of measured position as a consequence of the rigidity of the surface are appreciated, most of all at the beginning of the experiments. As it can be seen, the stiffness of the three experiments stabilizes at a constant value of 1727.7 N/m for experiments 1 and 2, and 1691.5 N/m for the third experiment. High values of the stiffness value are due to the high rigidity of the surface.

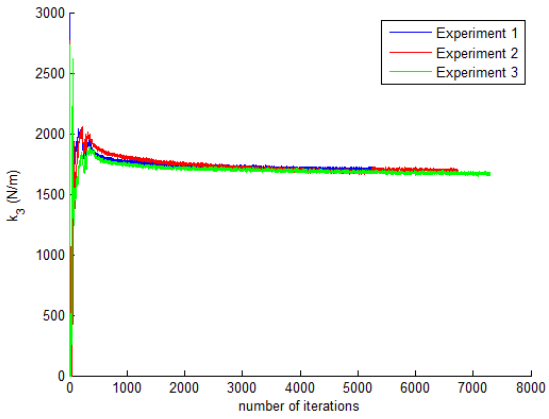

Figure 9. Third diagonal of the stiffness matrix estimation

C. Experimental results

The experiment consists on displacing the camera robot 75 mm along the y direction while exerting a force of 15 N on the surface simulating the abdominal wall. Sampling time is 0.002 seconds for the controllers, and 0.01 seconds for the rest of the scheme. System time constant of the first order behavior imposed to the robot dynamics is $\tau = 0.01$ seconds. PI gains in the position controller are $K_P = 10.0333$ and $K_I = -5.5167$. And gains of torque compensation and orientation controllers are $K_\tau = 100$ and $K_q = 150$.

Fig. 10 shows position, force and torque references tracking. Movement along the y direction is done following a trapezoidal velocity profile, with maximum velocity of 0.05 m/s, to obtain a smooth movement. As it can be observed in Fig. 10 (a), tracking of position reference is done accurately with a small delay during the transient-state. On the other hand, penetration on the surface is done following a linear profile, as it can be appreciated in the force response in Fig. 10 (b). Force and torque errors are mainly due to the inaccuracies of the force-torque sensor, which has an output resolution of 12 bits, with a noise of 2 bits. Fig. 10 (c) shows that torque norm starts with a null value when there is no contact with the surface, and then stabilizes at around 0.3 N/m when force reaches the steady-state at the desired force.

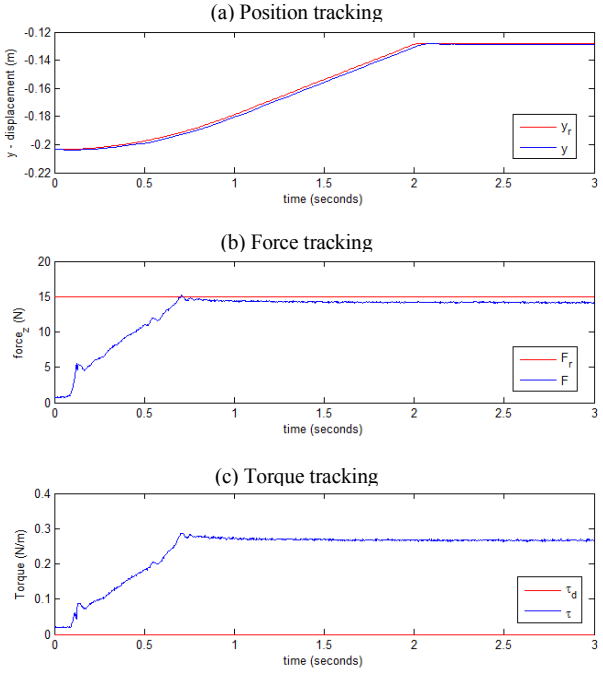

Figure 10. Position (a), force (b) and torque (c) references tracking

V. Conclusion

The robotic vision system proposed in this work represents a solution to the loss of triangulation due to the proximity of the camera and the surgical tools in single-sites

procedures. A first prototype of the wireless camera robot, 12 cm length by 4 cm width, has been designed and constructed. Future prototype designs will be targeted to reduce the overall size the robot. A LEDs lighting system is embedded into the robot to illuminate the operation area. Guidance of the robot along the abdominal wall is done by magnetic interaction with an external magnetic holder, which is attached to the end effector of a robotic arm. A hybrid position-force control has been proposed in order to displace the manipulator along the abdominal wall, while exerting a certain force on it. A torque compensation module has been included in the control scheme to maintain the end effector orientation perpendicular to the contact surface. To model the interaction between the manipulator and the environment, the abdominal wall has been assumed to be an elastic model. A recurrent least squares algorithm has been used to estimate the stiffness constant value. Finally, an in-vitro experiment has been carried out in order to validate the control scheme proposed. Future work will include experiments with different contact surfaces to check the feasibility of using the camera-guidance method proposed in a real minimally invasive operation.

REFERENCES

[1] J.R. Romanelli, L. Mark and P.A. Omotosho, "Single port laparoscopic cholecystectomy with the TriPort system: a case report," *Surgical Innovation*, vol. 15, no. 3, pp: 223-228, 2008.

[2] S.R. Philipp, B.W. Miedema, and K. Thaler, "Single-incision laparoscopic cholecystectomy using conventional instruments: early experience in comparison with the gold standard," *J. American College of Surgeons*, Vol. 209, No. 5, pp. 632-637, 2009.

[3] P. Bucher, F. Pugin, and P. Morel, "Single port access lapaoscopic right hemiclectomy," *Int. J. Colorectal Dis.*, vol. 23, pp. 1013-1016, 2010.

[4] D.R. Cox, W. Zeng, M.M. Frisella and L.M. Brunt, "Analysis of standard multiport verus single-site access for laparoscopic skills training," *Surgical Endoscopy*, vol. 25, pp. 1238-1244, 2011.

[5] L. Ott, Ph. Zanne, Fl. Nageotte, M. de Mathelin, and J. Gangloff, "Physiological motion rejection in flexible endoscopy using visual servoing," *IEEE Int. Conf. Robotics and Automation*, Pasadena, CA, USA, May 19-23, 2008, pp. 2928-2933.

[6] V. Karimyan, M. Sodergren, J. Clark, G.Z. Yang and A. Darzi, "Navigation systems and platforms in natural orifice translumenal endoscopic surgery (NOTES)," *Int. J. Surgery*, vol. 7, no. 4, pp. 297-304, 2009.

[7] T. Hu, P.K. Allen, N.J. Hogle and D.L. Fowler, "Insertable surgical imaging device with pan, tilt, zoom and lighting," *IEEE Int. Conf. Robotics and Automation*, May 2008, pp. 2948-2953.

[8] T. Kawahara, T. Takaki, I. Ishii and M. Okajima, "Development of a broad-view camera system for minimally invasive surgery," *IEEE/RSJ Int. Conf. Intelligent Robots and Systems*, October 2010, pp. 2810-2815.

[9] C.A. Castro, S. Smith, A. Alqassis, T. Ketterl, Y. Sun, S. Ross, A. Rosemurgy, P.P. Savage and R.D. Gitlin, "MARVEL: a wireless miniature anchored robotic videoscope for expedited laparoscopy," *IEEE Int. Conf. Robotics and Automation*, RiverCentre, May 2012, pp. 2926-2931.

[10] Y. Sun, A. Anderson, C. Castro, B. Lin, R. Gitlin, S. Ross and A. Rosemurgy, "Virtually transparent epidermal imagery for laparo-endoscopic single-site surgery," *33rd Annual Int. Conf. of the IEEE EMBS*, 2011, pp. 2107-2110.

[11] I. S. Zeltser, R. Bergs, R. Fernandez, L. Baker, R. Eberhart and J. A. Cadeddu, "Single trocar laparoscopic nephrectomy using magnetic anchoring and guidance system in the porcine model," *J. Urol.*, vol. 178, pp. 288–291, 2007.

[12] Valdastri P, Quaglia C, Buselli E, Arezzo A, Di Lorenzo N, Morino M, Menciassi and P. Dario, "A magnetic internal mechanism for precise orientation of the camera in wireless endoluminal applications," *Endoscopy*, vol. 42, no. 6, pp. 481-486, 2010.

[13] J. A. Cadeddu, R. Fernandez, M. Desai, R. Bergs, C. Tracy, S. J. Tang,P. Rao, M. Desai and D. Scott, "Novel magnetically guided intraabdominal camera to facilitate laparoendoscopic single-site surgery: Initial human experience," *Surgical Endoscopy*, vol. 23, pp. 1894–1899, 2009.

[14] M. Fakhry, B. Gallagher, F. Bello and G. B. Hanna, "Visual exposure using single-handed magnet-driven intra-abdominal wireless camera in minimal access surgery is better than 30◦ endoscope," Surgical Endoscopy, vol. 23, pp. 539–543, 2009.

[15] P. Swain, R. Austin, K. Bally and R. Trusty, "Development and testing of a tethered, independent camera for notes and single-site laparoscopic procedures," *Surgical Endoscopy.*, vol. 24, pp. 2013–2021, 2010.

[16] S. R. Platt, J. A. Hawks, and M. E. Rentschler, "Vision and task assistance using modular wireless in vivo surgical robots," *IEEE Trans. Biomedical Engineering*, vol. 56, no. 6, pp. 1700–1710, 2009.

[17] M. Nokata, S. Kitamura and T. Nakagi, "Capsule type medical robot with magnetic drive in abdominal cavity," *Proc. 2nd Biennial IEEE/RAS-WMBS Int. Conf. Biomedical Robotics and Biomechatronics*, pp. 348-353, 2008.

[18] F. Carpi, N. Kastelein, M. Talcott and C. Pappone, "Magnetically controllable gastrointestinal steering of video capsules," *IEEE Trans. Biomedical Engineering*, vol. 58, no. 2, pp. 231-234, 2011.

[19] A.C. Lehman, J. Dumpert, N.A. Wood, L. Redden, A.Q. Visty, S. Farritor, B. Varnell, and D. Oleynikov, "Natural orifice cholecystectomy using a miniature robot," *Surgical Endoscopy J.*, vol. 23, pp. 260-266, 2009.

[20] M. Simi, M. Silvestri, C. Cavallotti, M. Vatteroni, P. Valdastri, A. Menciassi and P. Dario, "Magnetically Activated Stereoscopic Vision System for Laparoscopic Single-Site Surgery," *IEEE/ASME Trans. Mechatronics*, vol. 18, no.3, pp. 1140-1151, June 2013

[21] S. Tognarelli, M. Salerno, G. Tortora, C. Quaglia, P. Daria and A. Menciassi, "An endoluminal robotic platform for minimally invasive surgery," *4th IEEE RAS/EMBS Int. Conf. Biomedical Robotics and Biomechatronics*, pp. 7-12, June 2012.

[22] B.S. Terry, Z.C. Mills, J.A. Schoen and M.E. Rentschler, "Single-Port-Access Surgery with a Novel Magnet Camera System," *IEEE Trans. Biomedical Engineering*, vol. 59, no. 4, April 2012.

[23] V.F. Muñoz, I. García-Morales, C. Perez del Pulgar, J.M. Gomez-DeGabriel, J. Fernández-Lozano, A. García-Cerezo, C. Vara-Thorbeck and R. Toscano, "Control movement scheme based on manipulability concept for a surgical robotic assistant," *IEEE Int. Conf. Robotics and Automation*, pp. 245-250, May 2006.

[24] H.L. Pham, V. Perdereau, B.V. Adorno and P. Fraisse, "Position and orientation control of robot manipulators using dual quaternion feedback," *IEEE/RSJ Int. Conf. Intelligent Robots and Systems*, pp. 658-663, October 2010.

[25] T. Barrera, A. Hast and E. Bengtsson, "Incremental Spherical Linear Interpolation", *SIGRAD 2004 Conf.*, pp. 7-10, November 2004.

[26] B. Rooks, "The harmonious robot" *Industrial Robot: An Int. J.*, vol. 33, no. 2, pp. 125–130, 2006.

[27] Barrett Technology, "F/T Sensor" (last access: July 2013). [Online]. Available: http://www.barrett.com/robot/DS_FTSENSOR.pdf

[28] E. Bauzano, V.F. Muñoz, I. García-Morales and B. Estebanez, "Three-layer control for active wrists in robotized laparoscopic surgery," *IEEE/RSJ Int. Conf. Intelligent Robots and Systems*, pp. 2653-2658, October 2009.

[29] M. Quigley, K. Conley, B. Gerkey, J. Faust, T.B. Foote, J. Leibs, R. Wheeler and A.Y. Ng, "ROS: an open-source Robot Operating System," *Int. Conf. Robotics and Automation*, ser. Open-Source Software workshop, 2009.